American Mineralogist, Volume 82, pages 337–344, 1997

Redox conditions in piston-cylinder apparatus: The different behavior of boron nitride and unfired pyrophyllite assemblies

JÜRGEN TRUCKENBRODT, DIETER ZIEGENBEIN, AND WILHELM JOHANNES

Institut für Mineralogie, Universität Hannover, Welfengarten 1, D-30167 Hannover, Germany

ABSTRACT

Piston-cylinder experiments with C-H-O fluids in equilibrium with graphite as redox sensor were performed at 900 °C and 10 kbar. With this technique, it is possible to investigate the hydrogen permeability of the material surrounding the samples and to determine the hydrogen fugacity. The furnace assembly consisted of boron nitride or unfired pyrophyllite.

Solid organic compounds ($C_4H_4O_4$, $C_9H_{10}O_2$, and $C_{14}H_{22}O$) were used as starting materials. The different H/O ratios of these compounds (1:1, 5:1, 22:1) result in different initial hydrogen fugacities. The fluid formed during the experiments was analyzed by gas chromatography.

The experimental data demonstrate that boron nitride is nearly impermeable to hydrogen at the investigated conditions. The hydrogen fugacity observed in the gold capsules is controlled by the composition of the C-H-O starting compound. After approximately 1 h it is 340 bar for experiments with $C_4H_4O_4$, 2400 bar for experiments with $C_9H_{10}O_2$, and 3200 bar for experiments with $C_{14}H_{22}O$ and remains constant for at least 8 d.

The situation is different with unfired pyrophyllite as the pressure-transmitting material. In these experiments, the same hydrogen fugacity was determined irrespective of the compositions of the organic compounds. The hydrogen fugacity seems to be controlled only by the furnace assembly. It is approximately 470 bar after 3 d.

The hydrogen fugacity in two samples placed side-by-side in the boron nitride assembly and containing different starting compounds (H/O = 1 and 5) becomes identical during experimental durations of less than 2 d. This is because of the exchange of hydrogen through the adjacent capsule walls. This observation can be used to measure the hydrogen fugacity of any piston-cylinder experiment. In boron nitride assemblies, a second capsule with a C-H-O fluid and graphite can also be applied to control the hydrogen fugacity within given limits.

INTRODUCTION

In high-pressure high-temperature experiments it is often required to know, or to control, the redox state of the investigated system. The oxygen fugacity (f_{O_2}) or the hydrogen fugacity (f_{H_2}) are commonly used to describe the redox state. Oxygen and hydrogen fugacity are related by the H_2O forming reaction:

$$H_2 + \frac{1}{2}O_2 \rightleftharpoons H_2O \qquad (1a)$$

$$\text{with } K_1 = \frac{f_{H_2O}}{f_{H_2} \cdot f_{O_2}^{1/2}} \qquad (1b)$$

where f_i is the fugacity of gas species i and K_1 is the equilibrium constant. The double-capsule technique (Eugster 1957) is a convenient way to control the f_{O_2}. Using this technique, the sample is sealed in an inner capsule, commonly consisting of either platinum or one of the Ag-Pd alloys, both highly permeable to hydrogen (Chou 1986). This capsule, together with a solid oxygen buffer assemblage and water, is in turn sealed in a larger outer capsule, made commonly of either gold or silver, which are relatively impermeable to hydrogen. For a given pressure and temperature f_{O_2} is fixed by the solid buffer, e.g., the Ni-NiO buffer mixture:

$$Ni + \frac{1}{2}O_2 \rightleftharpoons NiO \qquad (2a)$$

$$\text{with } K_2 = \frac{a_{NiO}}{a_{Ni} \cdot f_{O_2}^{1/2}} \qquad (2b)$$

where a_i is the activity of solid i and K_2 is the equilibrium constant. According to the H_2O-forming reaction (see Equations 1a and 1b), f_{H_2} is also fixed. f_{O_2} inside and outside of the inner capsule is the same, if the fluids on both sides have the same compositions. If the compositions of the fluids are different, f_{O_2} may be different, but f_{H_2} approaches the same value inside and outside the inner capsule if its wall is an effective hydrogen membrane.

However, in the case of piston-cylinder experiments the

0003–004X/97/0304–0337$05.00

small sample volume inside the furnace assembly limits the capacity of the oxygen buffer. At high temperatures, gold and silver are also effective hydrogen membranes (Chou 1986). If the redox state surrounding the double capsule is very different from the equilibrium redox state of the oxygen buffer, buffered experiments can be performed with relatively short experimental durations only. Therefore, several other methods were used to influence or estimate the redox conditions in the furnace assembly.

Different pressure-transmitting materials surrounding the sample may prevent hydrogen exchange between sample and furnace assembly. Rosenbaum and Slagel (1995) examined the effects of packing materials on hydrogen infiltration into sample capsules during piston-cylinder experiments. When soft glass or Pyrex completely enclosed a sample, it was effective at maintaining a low-hydrogen environment within the sample volume. They performed the experiments at 900 °C and pressures of 8 and 12.5 kbar with a platinum sample container. $BaCO_3$ was used as pressure-transmitting material in addition to Pyrex. Rushmer (1991) used solid media assemblies of talc and Pyrex sleeves with additional powdered Pyrex surrounding gold capsules. The powdered Pyrex helped to slow hydrogen diffusion during the experiments, which were performed at 800–1000 °C and 8 kbar. The oxygen fugacity in the sample was assumed to be close to that imposed by the quartz+fayalite+magnetite+H_2O (QFM) buffer. Frost and Wood (1995) used a double-capsule assembly to prevent hydrogen diffusion into the sample capsule. The sample container, together with CuO, was sealed in a larger platinum capsule. The CuO acted as a hydrogen "getter" by oxidizing H_2 to H_2O. The hydrogen fugacity in the sample capsule was effectively buffered at very low levels. A salt-borosilicate glass-graphite assembly was used for the experiments performed at 1100–1400 °C and 15–30 kbar.

Special capsule materials may also influence the redox state of the system. Hensen and Green (1971) loaded the samples into graphite capsules to eliminate the possibility of Fe loss to platinum containers and to retain conditions of low f_{O_2}. The experiments were performed at 800–1100 °C and 3.6–11.7 kbar in a furnace assembly with talc or boron nitride sleeves. Ellis and Green (1979) used graphite capsules at 1200 °C and 30 kbar or graphite capsules sealed with water inside large $Ag_{75}Pd_{25}$ containers at 750–900 °C and 15–30 kbar to avoid Fe loss and low f_{O_2}. Initial experiments of Ellis and Green (1979) were performed at 30 kbar in iron capsules, which maintained a lower oxygen fugacity than those performed in graphite capsules. The pressure-transmitting materials were talc and fired pyrophyllite. Takahashi and Kushiro (1983) performed piston-cylinder experiments at 1150–1600 °C and 5–35 kbar. Their samples were encased in graphite capsules, which were sealed in platinum containers. The oxygen fugacity of the experimental charge in a graphite capsule was believed to be within the stability field of wüstite at the applied experimental conditions.

Allen et al. (1972, 1975), Carroll and Wyllie (1989, 1990), Patiño Douce and Johnston (1991), Patiño Douce et al. (1993), Patiño Douce and Beard (1994, 1995), and Wolf and Wyllie (1994) observed that the furnace assembly may buffer the oxygen fugacity. Allen et al. (1972) performed experiments at 850–1100 °C and 10–26 kbar in a talc-graphite furnace assembly, modified for high temperatures by surrounding the capsule with BN. They determined that the samples (sealed in Ag-Pd capsules) were at oxygen fugacities close to those of the Ni+NiO+H_2O (NNO) buffer. Allen et al. (1975) confirmed this observation in experiments performed at 850–1155 °C and 10–36 kbar. They placed samples sealed in $Ag_{50}Pd_{50}$ capsules in a notched top surface of a BN cylinder. This cylinder overlaid a talc cylinder and a pyrophyllite disk. Carroll and Wyllie (1989, 1990) estimated the redox state of experiments performed in a graphite-NaCl assembly. They carried out experiments at 850–1100 °C and 15 kbar with a mixture of synthetic magnetite solid solution + ilmenite solid solution + H_2O in gold capsules, which yielded coexisting iron titanium oxide compositions indicating an f_{O_2} of about 0.5 log units above the NNO equilibrium. This was confirmed by Wolf and Wyllie (1994) using the same assembly. Patiño Douce and Johnston (1991) performed experiments at temperatures between 825 and 1075 °C and at pressures between 7 and 13 kbar. Two kinds of solid-medium cell assemblies were used, an all-NaCl cell up to about 20 °C below the melting point of NaCl and, at higher temperatures, a cell with $BaCO_3$ inner parts. Samples were enclosed in welded gold capsules. The oxide-mineral assemblage in most of the experiments employing the all-NaCl cell showed that the amount of Fe^{3+} in most of the charges was small, consistent with an oxygen fugacity in neighborhood of the QFM buffer. To compare the oxidation conditions imposed by the $BaCO_3$ cell with those obtained with the NaCl cell, they duplicated an experiment at 975 °C and 10 kbar with both assemblies. The oxide phase composition in the experiment with the $BaCO_3$ cell suggested an oxygen fugacity about 1.5 log units higher than that imposed by the NaCl cell. Patiño Douce et al. (1993) observed that the mineral assemblage in the experimental products and the garnet compositions are consistent with an f_{O_2} at or below the QFM buffer. They used a graphite-NaCl cell at temperatures between 825 and 975 °C and pressures between 7 and 13 kbar. The samples were welded shut in gold capsules. Patiño Douce and Beard (1994) performed piston-cylinder experiments in the range 925–1000 °C and 7–15 kbar in gold capsules. They used two kinds of solid-medium assemblies, a NaCl-graphite assembly and a $BaCl_2$-graphite assembly at 1000 °C and 10 kbar. The authors calculated an f_{O_2} below QFM using the orthopyroxene+hematite+quartz equilibrium. Patiño Douce and Beard (1995) confirmed this calculation with help of an additional oxygen-sensitive indicator, the biotite+ilmenite equilibrium. The log f_{O_2} was calculated to be between QFM and QFM−2.

However, the exact redox state of the system is not

known in the above mentioned investigations. It may be doubted whether these estimates can be transferred to modified furnace assemblies. Therefore, we have used C-H-O fluids in equilibrium with graphite as a redox sensor at 900 °C and 10 kbar. The hydrogen fugacity of an experiment can be calculated with help of the analyzed fluid. Furnace assemblies were BN and unfired pyrophyllite and we tried to find out if there is a pronounced hydrogen exchange between the sample and these assemblies.

Thermodynamic considerations

The system C-H-O

The number of degrees of freedom f in a system consisting of c components and p phases, can be expressed by the Gibbs phase rule, $f = c - p + 2$. The graphite-saturated system C-H-O ($a_C = 1$; a_C: activity of graphite) consists of three components (C, H, O) and two phases (fluid, assumed to be homogeneous, and graphite) and consequently has three degrees of freedom. If pressure and temperature are fixed, the variance is 1 and only one additional variable needs to be fixed, e.g., f_{H_2}. In a cold-seal apparatus this is often achieved by means of solid oxygen buffers such as NNO. The composition of the fluid is a function of the redox state of the system that can be described by f_{O_2}, f_{H_2}, or the atomic ratio H/O of the fluid. For a fluid consisting of the gas species H_2, CO_2, CH_4, CO, C_2H_6, and H_2O, the H/O ratio can be calculated by the following equation (x_i is the mole fraction of gas species i):

$$\frac{H}{O} = \frac{2 \cdot x_{H_2} + 4 \cdot x_{CH_4} + 6 \cdot x_{C_2H_6} + 2 \cdot x_{H_2O}}{2 \cdot x_{CO_2} + x_{CO} + x_{H_2O}} \quad (3)$$

Relations between hydrogen fugacity and H/O of the fluid

The redox state of a system is often given by f_{O_2}, which is related to f_{H_2} by the H_2O-forming reaction (see Equations 1a and 1b). Because the composition of the fluid surrounding the capsule is not known, f_{O_2} inside and outside the sample container may be different, but f_{H_2} approaches the same value inside and outside the sample container. To avoid misunderstandings, in this paper we only use f_{H_2} to describe the redox state of the system.

The hydrogen fugacity is calculated from the measured H/O of the fluid with help of the computer program COH-MIX (Krautheim et al. 1992). In this program, fugacity coefficients, compressibility factors, and mixing rules are used to describe the real behavior of the pure species and the interactions among the different species in the fluid. Krautheim (1993) performed experiments at temperatures from 900 to 1100 °C in the pressure range 10 to 15 kbar to find out the best correspondence between experimental data and calculated values. The best agreement was obtained by comparison of the experimental results with the data predicted by the MCRK (modified compensated Redlich Kwong) calculation. The MCRK calculation is based on the CORK (compensated Redlich Kwong) equation of state (Holland and Powell 1991), which is combined with the mixing rules of De Santis et al. (1974) and the correction of Flowers (1979). Figure 1 illustrates that the fluid composition is a function of the H/O of the fluid. The H/O describes the fluid composition unambiguously. Figure 2 indicates the calculated dependence of the H/O on the hydrogen fugacity.

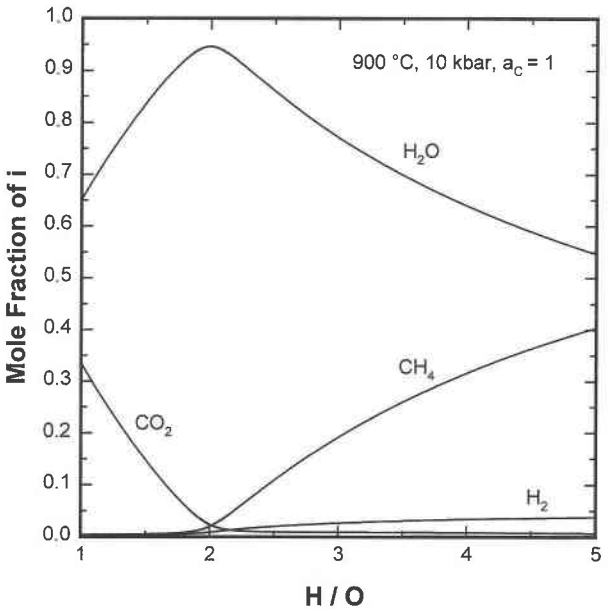

Figure 1. Fluid composition vs. H/O of the fluid. The fluid composition is computed with help of the MCRK-calculation (for details, see text). The mole fractions of CO and C_2H_6 are below 0.01. All calculations were made for 900 °C, 10 kbar, and an activity of graphite (a_C) = 1.

Experimental methods

Starting materials and sample preparation

Three different solid organic compounds, stored in a silica-gel desiccator, were used as starting materials: (1) fumaric acid ($C_4H_4O_4$, Merck No. 800269), starting H/O = 1; (2) 4′-acetophenone ($C_9H_{10}O_2$, Merck No. 805795), starting H/O = 5; and (3) 4-(1,1,3,3-Tetramethyl-butyl)-phenol $C_{14}H_{22}O$, Merck No. 806904), starting H/O = 22.

Approximately 3–5 mg of one of these compounds was loaded into gold capsules of the following dimensions: outer diameter 3.2 mm, inner diameter 2.8 mm, length 10 mm. The capsules were then flattened and welded shut. Efficient cooling during welding was achieved by dipping the sample capsules into water. After the experiment, oxygen balance was calculated from the analytical data to make sure that no weight loss had occurred during welding.

Experimental procedures

A piston-cylinder apparatus of the type described by Johannes (1973) was used throughout this study. The fur-

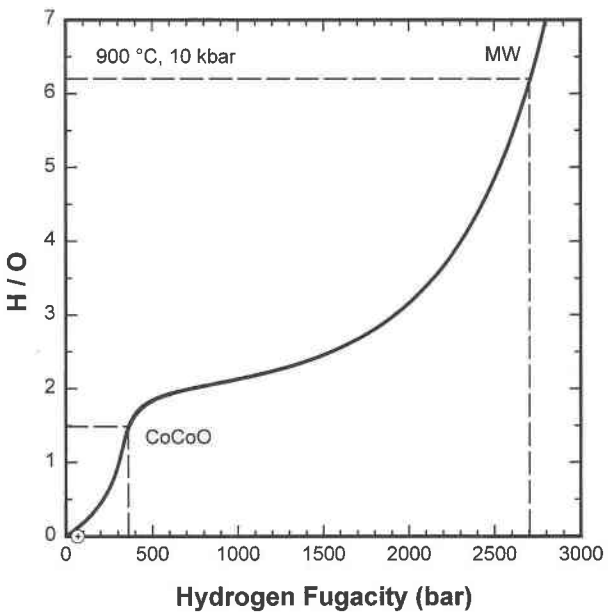

FIGURE 2. H/O of fluids vs. f_{H_2}. The relation between H/O and hydrogen fugacity (solid line) is computed with help of the MCRK-calculation (for details, see text). The calculations were made for 900 °C, 10 kbar, and an activity of graphite (a_C) = 1. The dashed lines represent the hydrogen fugacities imposed by the Co+CoO+H_2O (CoCoO) and magnetite+wüstite+H_2O (MW) buffer equilibria, respectively, and the corresponding H/O of the fluids in the sensor capsules.

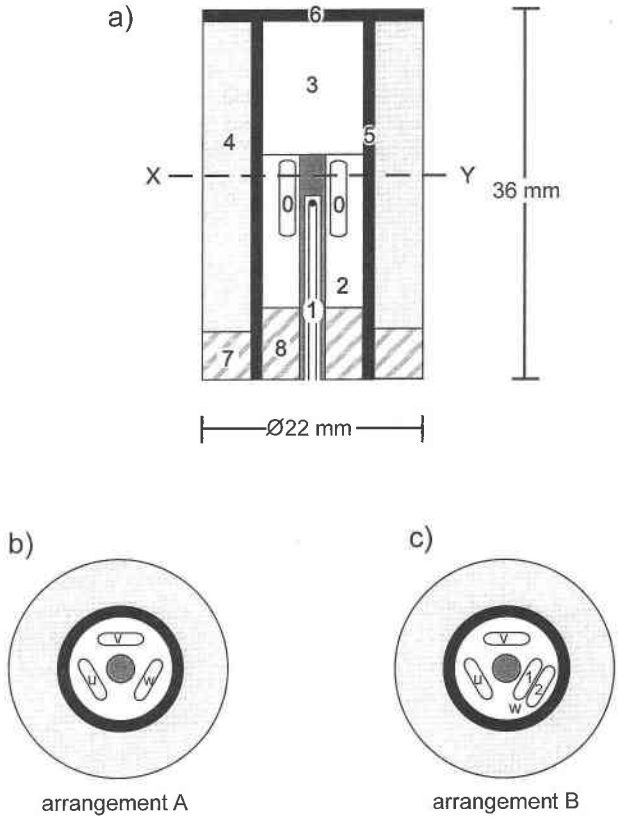

FIGURE 3. Set up of the high-pressure cell. (**a**) Vertical section of the high pressure cell. 0: samples; 1: thermocouple surrounded by a metal tube; 2+3: BN or unfired pyrophyllite; 4: NaCl; 5: graphite furnace; 6: graphite disk; 7: fired pyrophyllite; 8: unfired pyrophyllite. X-Y: horizontal sections. (**b**) Horizontal section X-Y showing arrangement A. u, v, w: sample capsules. Each capsule has its own pocket. (**c**) Horizontal section X-Y showing arrangement B. u, v, w_1, w_2: sample capsules. The capsules u and v have own pockets. The capsules w_1 and w_2 are placed side-by-side in the third pocket.

nace assembly consisted of a graphite tube that was surrounded by a NaCl sleeve. Inside the tube the pressure-transmitting material surrounding the sample capsules was either BN (grade ASBN, purchased from Elektroschmelzwerk Kempten GmbH) or unfired pyrophyllite (Fig. 3). The BN is hot pressed, tension-free fired, and cleaned with methanol. In the lower cylinder (part 2 in Fig. 3a) three pockets were drilled for the sample capsules. During the first set of experiments only one capsule was located in each pocket (u, v, w in Fig. 3b; arrangement A). In a second set of experiments this arrangement was modified. Two samples had their own pockets and two further samples were placed side-by-side in a third pocket (see arrangement B in Fig. 3c).

The temperature was controlled and measured by an Inconel-sheathed NiCr-Ni thermocouple (DIN IEC 584-1). No correction for pressure effects on EMF was applied. The thermal gradient over the sample position is supposed to be less than 5 °C (Johannes 1973). Temperature stability throughout all experiments was better than ± 5 °C. The temperature was controlled either by an Eurotherm-820 controller or a PCS-controller I. The piston-in method was applied (Johannes et al. 1971). The cold sample was exposed to a pressure of about 2 kbar below the final pressure. After the temperature of the experiment had been attained the pressure was raised to a value 0.5 kbar above the nominal pressure of the experiment. The pressure is considered accurate to ± 0.5 kbar (Johannes 1973). The experiments were terminated by turning off the current (initial quenching rate > 100 °C/s).

ANALYTICAL PROCEDURES

The fluid phase in the sample capsules was analyzed by gas chromatography. The analytical system consisted of two gas chromatographs (Shimadzu GC-8APT and GC-3BT), two temperature-programmed column ovens, and two thermal-conductivity detectors. With the help of two kinds of columns (molecularsieve 5A, Supelco cat. No. 2-0302, and Porapak Q, 80/100, Supelco cat. No. 2-0331) the gas species H_2, O_2, N_2, CO_2, CH_4, CO, C_2H_6, and H_2O could be separated and detected in only one analysis. The system was calibrated for a quantitative analysis of H_2, CO, and C_2H_6 with a minimum weight of 2 μg and of CO_2, CH_4, and H_2O with a minimum weight of 10 μg. The sample capsules were opened in vacuum in a heated capsule-puncturing system (Ziegenbein and Johannes 1977). This system was connected to the ana-

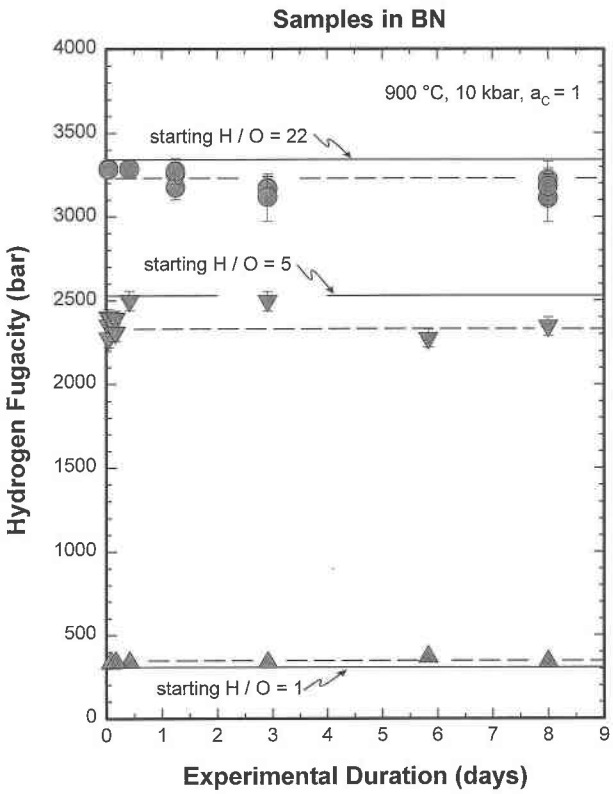

FIGURE 4. Hydrogen fugacity vs. experimental duration for different starting materials. Sample capsules were embedded in BN. Arrangement A was applied (each capsule had its own pocket). Apex-up triangles: $C_4H_4O_4$ (H/O = 1) used as starting material. Apex-down triangles: $C_9H_{10}O_2$ (H/O = 5) used as starting material. Circles: $C_{14}H_{22}O$ (H/O = 22) used as starting material. Dashed lines: Average hydrogen fugacities obtained in the capsules containing the same starting material. Solid lines: Hydrogen fugacities calculated for the starting H/O of 1, 5, or 22, respectively. All experiments were made at 900 °C and 10 kbar with an activity of graphite (a_C) = 1.

lytical system by a four-port valve. The capsules were examined optically to check that graphite was present.

EXPERIMENTAL RESULTS

Experiments performed with sample arrangement A

In the three pockets u, v, and w (Fig. 3b) either capsules with different or with the same starting materials ($C_4H_4O_4$: H/O = 1; $C_9H_{10}O_2$: H/O = 5; or $C_{14}H_{22}O$: H/O = 22) were placed. Each capsule had its own pocket. The capsules were surrounded by either BN or unfired pyrophyllite.

Capsules surrounded by BN. The initial hydrogen fugacity of experiments with a starting H/O of 1 is calculated to be 310 bar. During most of the experiments with such starting H/O the hydrogen fugacity increased and reached a value of 337 ± 3 bar, calculated from analyzed fluid composition (Fig. 4, Table 1). The hydrogen fugacity was practically constant between experimental durations of 2 and 192 h (Fig. 5).

TABLE 1. Arrangement A in BN parts: Experimentally determined H/O and calculated hydrogen fugacities

Starting H/O	Time (h)	Final H/O	f_{H_2} (bar)
1	2	1.25 ± 0.03	334 ± 3
1	2	1.29 ± 0.03	338 ± 3
1	4	1.28 ± 0.02	337 ± 2
1	4	1.30 ± 0.02	339 ± 2
1	10	1.29 ± 0.03	338 ± 3
1	70	1.27 ± 0.02	336 ± 2
1	140	1.51 ± 0.02	368 ± 4
1	192	1.31 ± 0.02	340 ± 2
5	1	4.18 ± 0.18	2350 ± 5
5	1	3.90 ± 0.17	2280 ± 7
5	1	4.38 ± 0.19	2400 ± 45
5	2	4.34 ± 0.19	2390 ± 45
5	4	4.34 ± 0.19	2390 ± 45
5	4	4.02 ± 0.18	2310 ± 52
5	10	4.85 ± 0.22	2500 ± 58
5	70	4.83 ± 0.22	2497 ± 58
5	140	3.89 ± 0.16	2273 ± 53
5	192	4.15 ± 0.17	2345 ± 54
22	1	18.61 ± 3.39	3289 ± 38
22	1	18.19 ± 3.24	3282 ± 38
22	10	18.51 ± 3.22	3287 ± 38
22	10	18.37 ± 3.04	3285 ± 38
22	30	16.89 ± 3.01	3255 ± 75
22	30	13.74 ± 3.07	3174 ± 73
22	30	17.74 ± 3.59	3273 ± 75
22	70	13.59 ± 2.93	3170 ± 73
22	70	13.42 ± 2.83	3164 ± 73
22	70	12.08 ± 2.76	3120 ± 142
22	192	15.36 ± 3.41	3220 ± 111
22	192	11.91 ± 2.80	3110 ± 142
22	192	13.91 ± 3.53	3180 ± 108

Note: All experiments were performed at 900 °C, 10 kbar with an activity of graphite = 1.

The initial hydrogen fugacity of experiments with a starting H/O of 5 is calculated to be 2530 bar. The hydrogen fugacity decreased during most of these experiments and adjusted to a value of about 2342 ± 62 bar, calculated from analyzed fluid composition (Fig. 4, Table 1). This decrease happened in the first hour. Between experimental durations of 1 and 192 h, there was no variation of the f_{H_2} (Fig. 5). During two experiments (10 and 70 h duration) the hydrogen fugacity was practically within the error of the initial value. Nearly the same hydrogen fugacity of about 2500 ± 58 bar was calculated from the analyzed fluid composition.

The initial hydrogen fugacity of experiments with a starting H/O of 22 is calculated to be 3340 bar. In experiments with this H/O the hydrogen fugacity decreased to a value of about 3216 ± 106 bar, calculated from analyzed fluid composition. The hydrogen fugacity was nearly constant between experimental durations of 1 and 8 d (Fig. 4, Table 1).

Capsules surrounded by unfired pyrophyllite. During one experiment three capsules with different starting materials (H/O = 1, H/O = 5, H/O = 22) were surrounded by unfired pyrophyllite. After a duration of 70 h the hydrogen fugacity in all three capsules was nearly the same. The hydrogen fugacity was about 507 ± 29 bar, calculated from the analyzed fluid composition (Table 2).

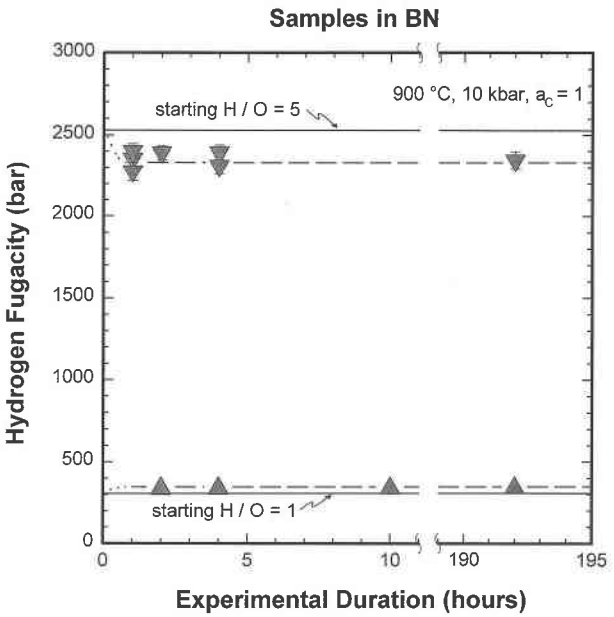

FIGURE 5. Hydrogen fugacity vs. experimental duration for different starting materials. Sample capsules were embedded in BN. Arrangement A was applied (each capsule had its own pocket). Apex-up triangles: $C_4H_4O_4$ (H/O = 1) used as starting material. Apex-down triangles: $C_9H_{10}O_2$ (H/O = 5) used as starting material. Dashed lines: Trends of time dependent variation of f_{H_2}. Solid lines: Hydrogen fugacities calculated for the starting H/O of 1 or 5. All experiments were made at 900 °C and 10 kbar with an activity of graphite (a_C) = 1.

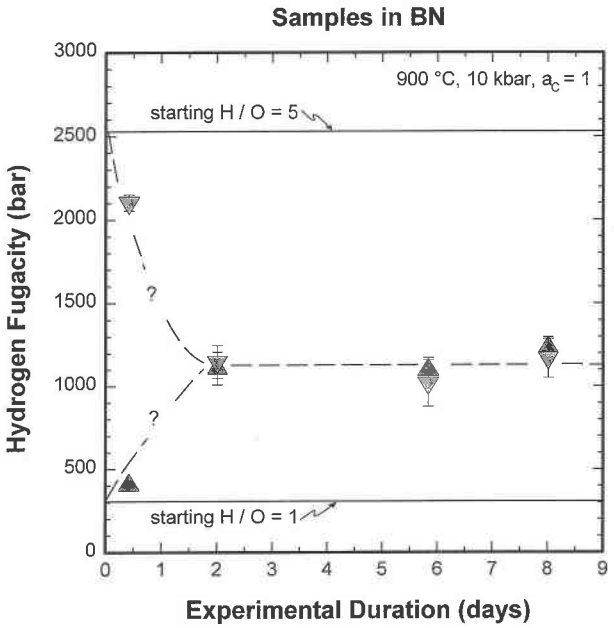

FIGURE 6. Hydrogen fugacity vs. experimental duration for different starting materials. Sample capsules were embedded in BN. Arrangement B was applied (two capsules with different starting materials placed side-by-side in the same pocket). Apex-up triangles: $C_4H_4O_4$ (H/O = 1) used as starting material. Apex-down triangles: $C_9H_{10}O_2$ (H/O = 5) used as starting material. Dashed lines: Trends of time dependent variation of hydrogen fugacity. Solid lines: Hydrogen fugacities calculated for the starting H/O of 1 or 5. All experiments were made at 900 °C and 10 kbar with an activity of graphite (a_C) = 1.

Experiments performed with sample arrangement B

Pocket u and v of arrangement B (Fig. 3c) contained one capsule filled with either $C_4H_4O_4$ (H/O = 1) or $C_9H_{10}O_2$ (H/O = 5). In pocket w two capsules (w_1, w_2) with different starting materials ($C_4H_4O_4$ or $C_9H_{10}O_2$) were placed side-by-side. The capsules were surrounded either by BN or unfired pyrophyllite.

Capsules surrounded by BN. The capsules located in pockets u and v of arrangement B confirm the results obtained already in experiments with arrangement A. The side-by-side samples w_1 and w_2 behaved different compared to those at isolated positions. After an experimental duration of 10 h the redox conditions in both capsules were still different (Fig. 6, Table 3). But after an experimental duration of 2 d the f_{H_2} in both capsules was the same and did not change in experiments of longer durations (up to 8 d). A comparison of the hydrogen contents present in the products with the H/O of 1 or 5 shows that almost all hydrogen that left the capsule with initial H/O of 5 is detected in the samples with initial H/O of 1 (e.g., in the 8 d experiment the capsule with the starting H/O of 5 lost 129 μmol hydrogen; in the capsule with a starting H/O of 1 an increase of 126 μmol hydrogen was observed), assuming that the hydrogen did not come from another source. The variation of the hydrogen content was

TABLE 2. Arrangement A in unfired pyrophyllite parts: Experimentally determined H/O and calculated hydrogen fugacities

Starting H/O	Time (h)	Final H/O	f_{H_2} (bar)
1	70	1.87 ± 0.05	531 ± 60
5	70	1.81 ± 0.04	478 ± 33
22	70	1.85 ± 0.04	511 ± 42

Note: All experiments were performed at 900 °C, 10 kbar with an activity of graphite = 1.

TABLE 3. Arrangement B in BN parts: Experimentally determined H/O of capsules placed side-by-side and calculated hydrogen fugacities

Starting H/O	Time (h)	Final H/O	f_{H_2} (bar)
1	10	1.66 ± 0.04	404 ± 13
1	48	2.19 ± 0.04	1122 ± 75
1	140	2.18 ± 0.04	1095 ± 75
1	192	2.25 ± 0.04	1227 ± 65
5	10	3.38 ± 0.15	2098 ± 48
5	48	2.20 ± 0.07	1148 ± 148
5	140	2.14 ± 0.07	1020 ± 139
5	192	2.21 ± 0.07	1160 ± 118

Note: All experiments were performed at 900 °C, 10 kbar with an activity of graphite = 1.

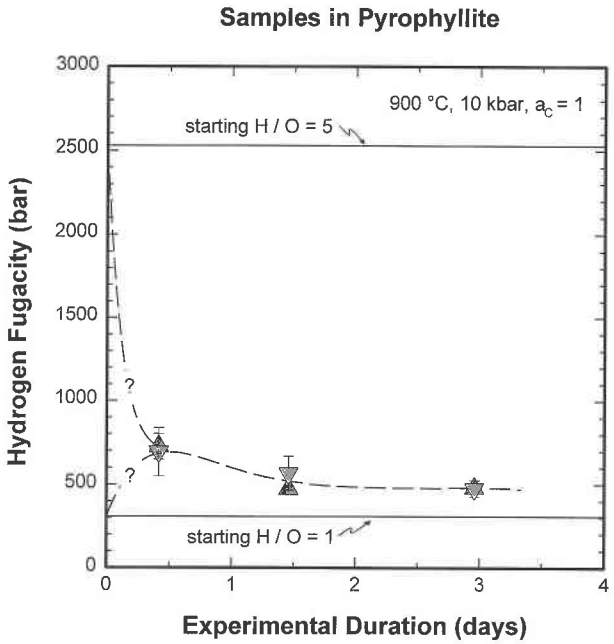

FIGURE 7. Hydrogen fugacity vs. experimental duration for different starting materials. Sample capsules were embedded in unfired pyrophyllite. Arrangement B was applied (two capsules with different starting materials placed side-by-side in the same pocket). Apex-up triangles: $C_4H_4O_4$ (H/O = 1) used as starting material. Apex-down triangles: $C_9H_{10}O_2$ (H/O = 5) used as starting material. Dashed lines: Trends of time dependent variation of hydrogen fugacity. Solid lines: Hydrogen fugacities calculated for the starting H/O of 1 or 5. All experiments were made at 900 °C and 10 kbar with an activity of graphite (a_C) = 1.

calculated by comparison of the hydrogen content of the starting material with the hydrogen content of the analyzed fluid.

Capsules surrounded by unfired pyrophyllite. After an experimental duration of 10 h in both capsules w_1 and w_2 placed side-by-side f_{H_2} was the same. The hydrogen fugacity was about 706 ± 16 bar, calculated from analyzed fluid composition (Fig. 7, Table 4). The hydrogen fugacity decreased in both samples with increasing duration of the experiment. After 3 d the hydrogen fugacity in both capsules decreased to a value of about 473 ± 2 bar. Isolated capsules having each their own pocket in unfired pyrophyllite (pockets u, v in Fig. 3c) filled with different starting materials (H/O = 1 or 5) yielded nearly the same f_{H_2} as observed in the capsules w_1 and w_2 placed side-by-side in one pocket (Table 4).

TABLE 4. Sample capsule arrangement B in unfired pyrophyllite parts: Experimentally determined H/O and calculated hydrogen fugacities

Starting H/O	Time (h)	Final H/O	f_{H_2} (bar)	Position in pyrophillite
1	71	1.69 ± 0.03	414 ± 10	u or v
5	71	1.81 ± 0.04	476 ± 28	u or v
1	10	2.00 ± 0.04	721 ± 76	w_1 or w_2
1	35	1.79 ± 0.04	468 ± 22	w_1 or w_2
1	71	1.80 ± 0.03	474 ± 16	w_1 or w_2
5	10	1.98 ± 0.08	690 ± 144	w_1 or w_2
5	35	1.90 ± 0.08	560 ± 101	w_1 or w_2
5	71	1.80 ± 0.07	471 ± 50	w_1 or w_2

Notes: All experiments were conducted at 900 °C, 10 kbar with an activity of graphite = 1; u or v—one capsule in one pocket; w_1 or w_2—two capsules placed side-by-side in one pocket.

DISCUSSION

The experimental data demonstrate that BN is nearly impermeable for hydrogen at the investigated conditions. A slight change in hydrogen contents of the capsules occurs only during the first hour if it happens at all (Fig. 5). In two experiments with an initial H/O of 5 and durations of 10 and 70 h only a very small loss of hydrogen was observed. Furthermore, one capsule with an initial H/O of 1 and a duration of 140 h showed a slightly larger increase in f_{H_2} in comparison with the other capsules containing the same starting material. Comparing experiments with an initial H/O = 1 with those with an initial H/O = 5 demonstrates that the increase of the hydrogen fugacity in the capsule with an initial H/O = 1 is big when the decrease in the capsule with an initial H/O = 5 is big or that the increase of the hydrogen fugacity in the capsule with an initial H/O = 1 is small when the decrease in the capsule with an initial H/O = 5 is small. The samples with H/O = 1 and H/O = 5 and the same duration of the experiment were treated in the same experiment (and BN parts; Fig. 4). The reason for this observation must be a different hydrogen permeability of the BN in the first hour of the experiment. This interpretation is also the only one that can explain why the hydrogen fugacities of capsules with an initial H/O of 5, determined after 10 and 70 h, are higher than those determined after 2 and 4 h. Therefore, we conclude that f_{H_2} of all experiments longer than 1 h is constant. The hydrogen fugacity observed in the capsule depends mainly on the composition of the starting material and slightly on the permeability of BN in the first hour of the experiments.

It could be observed that f_{H_2} in two capsules with different starting materials (H/O = 1 or 5) placed side-by-side in one pocket becomes identical during experimental durations of less than 2 d (Fig. 6). This observation is of practical importance and may be used to measure the hydrogen fugacity of any piston-cylinder experiment. An unknown hydrogen fugacity can be determined with the help of a second sensor capsule containing C-H-O fluid with graphite. Depending on the relative masses of hydrogen in the sample and in the sensor capsule, one must decide beforehand in which direction hydrogen is flowing to approach equilibrium. Different directions of hydrogen flow at the beginning of the experiments may influence the sample, e.g., influence the occurrence and stability of mineral phases. In BN assemblies, a second capsule with a C-H-O fluid and graphite added to a sample capsule

may also be used to influence the hydrogen fugacity in the sample in given limits.

Graphite-NaCl assemblies are supposed to buffer f_{O_2}. However, similar experimental setups are stated to yield very different oxygen fugacities. The oxygen fugacity varies from 0.5 log units above NNO (Carroll and Wyllie 1989,1990; Wolf and Wyllie 1994) to QFM or 2 log units below QFM (Patiño Douce and Johnston 1991; Patiño Douce et al. 1993; Patiño Douce and Beard 1994; 1995). The behavior of BN differs from these observations with NaCl assemblies. The redox conditions are not controlled by the furnace assembly, but depend on the composition of the starting material.

Unfired pyrophyllite seems to behave like NaCl. In all three pockets of pyrophyllite assemblies the same f_{H_2} was determined independently of the starting H/O in the sample. The furnace assembly seems to control f_{H_2}. After an experimental duration of approximately 1 d the hydrogen fugacity is the same in all capsules with different starting materials. However, the hydrogen fugacity did not remain constant, but decreased slightly with increasing duration of the experiment (see Fig. 7 and Table 4). This is approximately 100 bar above that of the Co+CoO+H_2O buffer (363 bar).

Acknowledgments

We thank Manfred Schliestedt for helpful comments and critical review of this paper. Many thanks also to Alberto Patiño Douce and John Dalton. The manuscript benefited significantly from their critical reviews. This work was supported by the German Science Foundation (DFG, Az. Jo 63/25-3).

References cited

Allen, J.C., Modreski, P.J., Haygood, C., and Boettcher, A.L. (1972) The role of water in the mantle of the Earth: The stability of amphiboles and micas. 24th International Geological Congress, 2, 231–240.

Allen, J.C., Boettcher, A.L., and Marland, G. (1975) Amphiboles in andesite and basalt: I. Stability as a function of P-T-f_{O_2}. American Mineralogist, 60, 1069–1085.

Carroll, M.R., and Wyllie, P.J. (1989) Experimental phase relations in the system tonalite-peridotite-H_2O at 15 kb; implications for assimilation and differentiation processes near the crust-mantle boundary. Journal of Petrology, 30, 1351–1382.

———(1990) The system tonalite-H_2O at 15 kbar and the genesis of calc-alkaline magmas. American Mineralogist, 75, 345–357.

Chou, I.M. (1986) Permeability of precious metals to hydrogen at 2 kb total pressure and elevated temperatures. American Journal of Science, 286, 638–658.

De Santis, R., Breedveld, G.J.F., and Pausnitz, J.M. (1974) Thermodynamic properties of aqueous gas mixtures at advanced pressures. Industrial and Engineering Chemistry, Process Design and Development, 13, 374–377.

Ellis, D.J., and Green, D.H. (1979) An experimental study of the effect of Ca upon garnet-clinopyroxene Fe-Mg exchange equilibria. Contributions to Mineralogy and Petrology, 71, 13–22.

Eugster, H.P. (1957) Heterogeneous reactions involving oxidation and reduction at high pressures and temperatures. Journal of Chemical Physics, 26, 1760–1761.

Flowers, G.C. (1979) Correction of Holloway's (1977) adaption of the modified Redlich-Kwong equation of state for calculation of fugacities of molecular species in supercritical fluids of geologic interest. Contributions to Mineralogy and Petrology, 69, 315–318.

Frost, D.J., and Wood B.J. (1995) Experimental measurements of the graphite C-O equilibrium and CO_2 fugacities at high temperature and pressure. Contributions to Mineralogy and Petrology, 121, 303–308.

Hensen, B.J., and Green, D.H. (1971) Experimental study of the stability of cordierite and garnet in pelitic compositions at high pressures and temperatures. Contributions to Mineralogy and Petrology, 33, 309–330.

Holland, T., and Powell, R. (1991) A Compensated-Redlich-Kwong (CORK) equation for volumes and fugacities of CO_2 and H_2O in the range 1 bar to 50 kbar and 100–1600 °C. Contributions to Mineralogy and Petrology, 109, 265–273.

Johannes, W. (1973) Eine vereinfachte Piston-Zylinder-Apparatur hoher Genauigkeit. Neues Jahrbuch für Mineralogie Monatshefte, 7/8, 337–351.

Johannes, W., Bell, P.M., Mao, H.K., Boettcher, A.L., Chipman, D.W., Hays, J.F., Newton, R.C., and Seifert, F. (1971) An interlaboratory comparison of piston-cylinder pressure calibration using the albite-breakdown reaction. Contributions to Mineralogy and Petrology, 32, 24–38.

Krautheim, J. (1993) Experimentelle Untersuchungen und thermodynamische Berechnungen zur Charakterisierung von Fluiden der unteren Erdkruste und des oberen Erdmantels. Thesis, Institute of Mineralogy, University of Hannover, Germany.

Krautheim, J., Johannes, W., and Ziegenbein, D. (1992) COH-MIX—Ein Programm zur Berechnung von COH-Fluiden. Beihefte zum European Journal of Mineralogy, 4, 158.

Patiño Douce, A.E., and Johnston, A.D. (1991) Phase equilibria and melt productivity in the pelitic system: Implications for the origin of peraluminous granitoids and aluminous granulites. Contributions to Mineralogy and Petrology, 107, 202–218.

Patiño Douce, A.E., Johnston, A.D., and Rice, J.M. (1993) Erratum. Octahedral excess mixing properties in biotite: A working model with applications to geobarometry and geothermometry. American Mineralogist, 78, 826.

Patiño Douce, A.E., and Beard, J.S. (1994) H_2O loss from hydrous melts during fluid-absent piston cylinder experiments. American Mineralogist, 79, 585–588.

———(1995) Dehydration-melting of biotite gneiss and quartz amphibolite from 3 to 15 kbar. Journal of Petrology, 36, 707–738.

Rosenbaum, J.M., and Slagel, M.M. (1995) C-O-H speciation in piston-cylinder experiments. American Mineralogist, 80, 109–114.

Rushmer, T. (1991) Partial melting of two amphibolites: Contrasting experimental results under fluid-absent conditions. Contributions to Mineralogy and Petrology, 107, 41–59.

Takahashi, E., and Kushiro, I. (1983) Melting of a dry peridotite at high pressures and basalt magma genesis. American Mineralogist, 68, 859–879.

Wolf, M.B., and Wyllie, P.J. (1994) Dehydration-melting of amphibolite at 10 kbar: The effect of temperature and time. Contributions to Mineralogy and Petrology, 115, 369–383.

Ziegenbein, D., and Johannes, W. (1977) Gaschromatographic analysis of experimental high pressure hydrothermal fluids. Neues Jahrbuch für Mineralogie Abhandlungen, 130, 145–149.

Manuscript received January 8, 1996
Manuscript accepted December 11, 1996